

IMPLICIT INTEGRATION FACTOR METHOD COUPLED WITH PADÉ APPROXIMATION STRATEGY FOR NONLOCAL ALLEN-CAHN EQUATION*

YUXIN ZHANG[†] AND HENGFEI DING[‡]

Abstract. The space nonlocal Allen-Cahn equation is a famous example of fractional reaction-diffusion equations. It is also an extension of the classical Allen-Cahn equation, which is widely used in physics to describe the phenomenon of two-phase fluid flows. Due to the nonlocality of the nonlocal operator, numerical solutions to these equations face considerable challenges. It is worth noting that whether we use low-order or high-order numerical differential formulas to approximate the operator, the corresponding matrix is always dense, which implies that the storage space and computational cost required for the former and the latter are the same. However, the higher-order formula can significantly improve the accuracy of the numerical scheme. Therefore, the primary goal of this paper is to construct a high-order numerical formula that approximates the nonlocal operator. To reduce the time step limitation in existing numerical algorithms, we employed a technique combining the compact integration factor method with the Padé approximation strategy to discretize the time derivative. A novel high-order numerical scheme, which satisfies both the maximum principle and energy stability for the space nonlocal Allen-Cahn equation, is proposed. Furthermore, we provide a detailed error analysis of the differential scheme, which shows that its convergence order is $\mathcal{O}(\tau^2 + h^6)$. Especially, it is worth mentioning that the fully implicit scheme with sixth-order accuracy in spatial has never been proven to maintain the maximum principle and energy stability before. Finally, some numerical experiments are carried out to demonstrate the efficiency of the proposed method.

Key words. Riesz derivative, Discrete maximum principle, Energy stability, Implicit integration factor method

AMS subject classifications. 65M06, 35B65

1. Introduction. In this paper, we focus on numerical analysis of the phase field models involving space nonlocality. More specifically, we consider the following space fractional Allen-Cahn equation

$$(1.1) \quad \partial_t u - \epsilon^2 \mathcal{L}^\gamma u = -F'(u) := f(u), \quad (x, t) \in \Omega \times (0, T],$$

with the initial condition

$$u(\mathbf{x}, 0) = u_0(\mathbf{x}), \quad \mathbf{x} \in \bar{\Omega},$$

and the homogeneous Dirichlet boundary condition

$$u(\mathbf{x}, t)|_{\partial\Omega} = 0, \quad t \in (0, T],$$

where the function $F(u)$ is bistable, e.g., $F(u) = \frac{1}{4}(u^2 - 1)^2$ represents a double-well potential. Here $\Omega \subset \mathbb{R}^d$ ($d = 1, 2, 3$) is an open and bounded Lipschitz domain, $u : \bar{\Omega} \times [0, \infty) \rightarrow \mathbb{R}$ is the unknown function, $\epsilon > 0$ is the interfacial parameter representing the width of the transition regions [1]. The operator \mathcal{L}_γ denotes the Riesz-type fractional derivative of order $\gamma \in (1, 2]$ in space, which is a typical example of nonlocal operators and the one-dimensional case is defined by [2]

$$(1.2) \quad \mathcal{L}^\gamma u(x) = \partial_{x,\Omega}^\gamma u(x) := -\frac{1}{2 \cos(\frac{\pi}{2}\gamma) \Gamma(2-\gamma)} \frac{d^2}{dx^2} \int_{\Omega} |x-s|^{1-\gamma} u(s) ds, \quad x \in \mathbb{R}.$$

*This work was partially supported by the National Natural Science Foundation of China (Grant Nos. 12461069, 11961057), the Science and Technology Project of Guangxi (Grant No. GuikeAD21220114).

[†]School of Mathematics and Statistics, Guangxi Normal University, Guilin 541006, China. (E-mail: zhangyuxin2006@163.com).

[‡]1.School of Mathematics and Statistics, Guangxi Normal University, Guilin 541006, China; 2.The Center for Applied Mathematics of Guangxi (GXNU), Guilin 541006, China; 3.Guangxi Colleges and Universities Key Laboratory of Mathematical Model and Application (GXNU), Guilin 514006, China. (E-mail:dinghf05@163.com).

In the two-dimensional and three-dimensional cases, the Riesz derivative can also be defined similarly, that is,

$$\mathcal{L}^\gamma u(x, y) = \left(\partial_{x, \Omega}^\gamma + \partial_{y, \Omega}^\gamma \right) u(x, y), \quad (x, y) \in \mathbb{R}^2,$$

and

$$\mathcal{L}^\gamma u(x, y, z) = \left(\partial_{x, \Omega}^\gamma + \partial_{y, \Omega}^\gamma + \partial_{z, \Omega}^\gamma \right) u(x, y, z), \quad (x, y, z) \in \mathbb{R}^3.$$

Similar to the integer-order Allen-Cahn equation, the space fractional equation (1.1), as a phase-field model, can also be viewed as an L^2 gradient flow with respect to the following fractional analog of the Ginzburg-Landau free energy functional

$$(1.3) \quad E(u) = \int_{\Omega} \left(F(u) - \frac{1}{2} \varepsilon^2 u \mathcal{L}^\gamma u \right) dx.$$

It is well-known that the exact solution of the Allen-Cahn equation (1.1) has two important properties [3], i.e., preserves the maximum principle and satisfy the energy dissipation property with time. More precisely, the first one means that if the initial value is constrained by the constant 1 in the L^∞ norm, then the entire solution will be constrained by 1, i.e.,

$$\|u_0(\mathbf{x})\|_{L^\infty} \leq 1 \Rightarrow \|u(\mathbf{x}, t)\|_{L^\infty} \leq 1 \text{ for all } (\mathbf{x}, t) \in \overline{\Omega} \times (0, T],$$

where the symbol $\|\cdot\|_{L^\infty}$ is the L^∞ norm and defined by $\|u\|_{L^\infty} = \max_{\mathbf{x} \in \overline{\Omega}} |u(\mathbf{x})|$. The second one implies that the corresponding energy functional (1.3) decreases over time, that is

$$\frac{d}{dt} E(u) = \left(\frac{\delta E(u)}{\delta u}, \phi(u) \right) = - \|\partial_t(\mathbf{x}, t)\|^2 \leq 0, \text{ for any } t > 0,$$

which is often called the nonlinear energy stability, where $\phi(u) = \varepsilon^2 \mathcal{L}^\gamma u + f(u)$, the symbols (\cdot, \cdot) and $\|\cdot\|$ are the standard inner product and L^2 norm, which are defined by

$$(u, v) = \int_{\Omega} uv dx, \quad \|u\|^2 = \int_{\Omega} |u|^2 dx, \quad \text{any } u, v \in L^2(\Omega).$$

Spatial nonlocal Allen-Cahn equation (1.1) is a partial differential equation, which extends the classical Allen-Cahn equation by introducing fractional derivative. The classic Allen-Cahn equation is one of the basic models to study phase transition and interface dynamics, especially material science and fluid dynamics. Because the nonlocal model introduces the fractional derivative term considering the long-range interaction, it is suitable for describing a wider range of phenomena. For example, nonlocal Allen-Cahn equation (1.1) can be used to simulate the dynamic behavior of cell populations or tissues, in which cell interactions over long distances can be represented by fractional derivatives. For example, in the tumor growth model, the fractional derivative can explain the influence of nutrient concentration or signal molecules on diffusion in a large range. In addition, this model can also be used to study the pattern formation process in biological tissues, such as the arrangement and combination of cells in developing embryos, in which long-range interaction plays a crucial role, that is, fractional derivatives play an important role. Unfortunately, due to the influence of nonlocal operators, the exact solution of model (1.1) is generally difficult to obtain, which has caused great obstacles to the further study of the dynamic behavior of the equation, so it is natural to seek an efficient numerical method as one of the best ways.

From equation (1.1), it is not difficult to find that in order to derive its efficient numerical algorithm, the first task is to construct the higher-order numerical differential formula of Riesz derivative. Generally speaking, there are two ways to construct the numerical differential formula of Riesz derivative, indirect method and direct method. In more detail, the former is to construct the numerical differential formulas of the left and right Riemann-Liouville derivatives first, and then sum them by weight. The latter is constructed from the definition itself. Up to now, some scholars have constructed a series of efficient numerical differential formulas in these two ways. In the direct method, the Grünwald–Letnikov formulas was used to approximate the Riemann-liouville derivatives in the early stage. Unfortunately, when it is applied to time-dependent spatial fractional differential equations, the numerical algorithm obtained is unstable. In order to make up for this shortcoming, Meerschaert and Tadjeran [4] proposed the so-called shifted Grünwald–Letnikov formula with convergence order of 1. Subsequently, Deng’s group put forward second-order and third-order numerical differential formulas by weighting and shifting Grünwald–Letnikov formulas [5, 6]. In order to improve stability and accuracy, Ding [7] also constructed a second-order numerical differential formula by constructing a new generation function. Looking back at the direct method, the most famous one is the second-order formula [8] based on the fractional central difference operator proposed by Ortigueira [9]. In recent years, higher-order formulas with this second-order formula as the core have also been obtained [10, 11, 12]. But as far as we know, numerical differential formulas with convergence order of 6 are still scarce.

Based on these numerical differential formulas mentioned above and their improvements and corrections, a large number of numerical algorithms have emerged for phase field models (1.1). Such as in [3], Hou et al. used the Crank-Nicolson method in time and second-order numerical differential formula by developed Tian et al. [5] in space, and constructed a difference scheme with order $\mathcal{O}(\tau^2 + h^2)$, which show that the numerical solution satisfied discrete maximum principle under $0 < \tau \leq \min\left\{\frac{1}{2}, \frac{h^\gamma}{2d\epsilon^2}\right\}$. Using the fourth-order numerical differential formula proposed by Ding and Li in [10], He et al. [13] constructed a spatial fourth-order operator splitting scheme for equation (1.1), and the discrete maximum principle was discussed under time step τ satisfies certain conditions. However, it is a pity that they do not give detailed theoretical proof for the error estimation and energy stability of the numerical scheme. In addition, from the numerical experiments given by them, it is not difficult to find that the energy is not always reduced, which reflects that the numerical scheme established does not always satisfy the energy dissipation property. In [14], Zhang et al. presented an implicit-explicit Runge-Kutta schemes with order $\mathcal{O}(\tau^p + h^2)$, where $p \geq 1$. And the discrete maximum principle, energy stability and error estimation were studied under the assumption of time step $0 < \tau \leq \frac{h^\gamma}{dg_0\epsilon^2}\tilde{\tau}$, where $g_0 = \frac{\Gamma(\gamma+1)}{\Gamma^2(\gamma/2+1)}$ and $\tilde{\tau}$ is a positive constant satisfying certain conditions. However, it is a little regrettable that the theoretical analysis of energy dissipation is not given in a strict sense, they only give the boundedness of discrete energy, which shows that the energy dissipation of the numerical solution is inconsistent with that of the exact solution. More recently, with the help of the symplectic Runge-Kutta method and the quadratic auxiliary variable technique [15] in time, and a fourth-order numerical differential formula developed by Hao et al. in [16] is applied to the space Riesz derivative. Xu and Fu [17] proposed a fully discretized implicit scheme with order $\mathcal{O}(\tau^2 + h^4)$, they analyzed the discrete energy stability and maximum principle under the condition $0 \leq \tau \leq \min\left\{\frac{1}{2+\delta}, \frac{1}{3}, \frac{h^\gamma}{2d\epsilon^2}\right\}$, where $0 \leq \delta \leq 4$. For more studies on equation (1.1), it can be found in references [18, 19, 20].

From above analysis, we can see that although there are some studies on the space fractional Allen-Cahn equation (1.1), it is still limited. Moreover, as far as we know, there is no numerical scheme whose spatial convergence order is higher than 4, and the condition of preserving the discrete maximum principle is independent of ϵ and h . Therefore, the main

motivation of our work in this paper is to make up for these shortcomings, so as to obtain an efficient numerical scheme for solving equation (1.1). Compared with existing researches, our contributions are listed as below.

- By constructing a new generating function, a sixth-order numerical differential formula for approximating the space Riesz derivative is established.
- The implicit integral factor method coupled with Padé approximation strategy is proposed to deal with the time derivative.
- The condition of preserving the maximum principle of the numerical scheme constructed in this paper is $0 < \tau \leq 1$, which is independent of the parameters ϵ and h , and significantly improves the condition of preserving the maximum principle of the numerical schemes in the existing literatures.
- The convergence order of our difference scheme can reach $\mathcal{O}(\tau^2 + h^6)$ in the sense of discrete maximum norm, which is obviously higher than the existing schemes.

The rest of this paper is organized as follows. In Section 2, we construct a new sixth-order numerical differential formula that approximates the Riesz derivative, and apply it to equation (1.1), thus obtaining a fully discrete finite difference scheme. In Section 3, the properties of the proposed difference scheme are studied in detail, including discrete maximum principle, discrete energy stability and convergence. Numerical experiments are presented to confirm the theoretical analysis and demonstrate the efficiency of the provided schemes in Section 4. The last section is concerned with the conclusion.

2. Numerical scheme. In this section, we first present a sixth-order numerical differential formula for the space Riesz derivative, and obtain the corresponding semi-discrete numerical scheme. Then a fully discrete scheme is proposed by applying the implicit integration factor method couple Padé approximation strategy in time.

2.1. Space discretization. Here, we apply a uniform partition of Ω into square elements of length h , and let M be the total number of grid nodes. In order to effectively approximate the Riesz derivative, we can construct a higher-order numerical differential formula by using the strategy of seeking suitable new generating functions. In the paper, we design a new generating function $G(w)$ with the following form

$$(2.1) \quad G(w) = (2 - w - w^{-1})^{\frac{\gamma}{2}} \left[1 + \frac{\gamma}{24} (2 - w - w^{-1}) + \frac{\gamma(5\gamma + 22)}{5760} (2 - w - w^{-1})^2 \right],$$

and it is analytic, that is

$$(2.2) \quad G(w) = \sum_{m=-\infty}^{+\infty} g_m^{(\gamma)} w^m, \quad |w| \leq 1.$$

Using a similar technique as in [21, 22], we know that the exact expression of the coefficient $g_m^{(\gamma)}$ is

$$(2.3) \quad \begin{aligned} g_m^{(\gamma)} &= \frac{1}{2\pi} \int_{-\pi}^{\pi} G(e^{is}) e^{-ims} ds \\ &= \frac{(-1)^m \Gamma(\gamma + 1)}{\Gamma(\frac{\gamma}{2} - m + 1) \Gamma(\frac{\gamma}{2} + m + 1)} \left[1 + \frac{\gamma(\gamma + 1)(\gamma + 2)}{6(\gamma - 2m + 2)(\gamma + 2m + 2)} \right. \\ &\quad \left. + \frac{\gamma(\gamma + 1)(\gamma + 2)(\gamma + 3)(\gamma + 4)(5\gamma + 22)}{360(\gamma - 2m + 4)(\gamma - 2m + 2)(\gamma + 2m + 4)(\gamma + 2m + 2)} \right], \quad m = 0, \pm 1, \dots \end{aligned}$$

Next, based on the above generating function (2.1), a new high-order numerical differential formula is constructed for approximating the Riesz derivative (1.2), and the main result is described in the following theorem.

THEOREM 2.1. *Suppose*

$$u \in \mathcal{C}^{6+\gamma}(\mathbb{R}) = \left\{ u \mid u \in L^1(\mathbb{R}), \text{ and } \int_{\mathbb{R}} (1+|s|)^{6+\gamma} |\hat{u}(s)| ds < \infty \right\}, \quad 1 < \gamma \leq 2,$$

where $\hat{u}(s)$ is the Fourier transform of $u(z)$ for all $s \in \mathbb{R}$. Then there holds that

$$\partial_{x,\mathbb{R}}^\gamma u(x) = \delta_{h,\mathbb{R}}^\gamma u(x) + \mathcal{O}(h^6)$$

uniformly as $h \rightarrow 0$, where the fractional difference operator $\delta_{h,\mathbb{R}}^\gamma$ is defined as

$$\delta_{h,\mathbb{R}}^\gamma u(x) = -h^{-\gamma} \sum_{m=-\infty}^{+\infty} g_m^{(\gamma)} u(x - mh).$$

Proof. Denote

$$(2.4) \quad \Phi(\varpi, h) = \mathcal{F} \left\{ \partial_{x,\mathbb{R}}^\gamma u(x) \right\} - \mathcal{F} \left\{ \delta_{h,\mathbb{R}}^\gamma u(x) \right\}.$$

Note that the Fourier transforms of the operators $\partial_{x,\mathbb{R}}^\gamma$ and $\delta_{h,\mathbb{R}}^\gamma$ are

$$\mathcal{F} \left\{ \partial_{x,\mathbb{R}}^\gamma \right\} = -|\varpi|^\gamma \hat{u}(\varpi),$$

and

$$\begin{aligned} \mathcal{F} \left\{ \delta_{h,\mathbb{R}}^\gamma u(x) \right\} &= -h^{-\gamma} \sum_{m=-\infty}^{+\infty} g_m^{(\gamma)} \mathcal{F} \left\{ u(x - mh), \varpi \right\} = -h^{-\gamma} \sum_{m=-\infty}^{+\infty} g_m^{(\gamma)} e^{im\varpi h} \hat{u}(\varpi) \\ &= -|\varpi|^\gamma \left[1 + \frac{\gamma}{6} \sin^2 \left(\frac{1}{2} \varpi h \right) + \frac{\gamma(5\gamma + 22)}{360} \sin^4 \left(\frac{1}{2} \varpi h \right) \right] \left| \frac{\sin \left(\frac{1}{2} \varpi h \right)}{\frac{1}{2} \varpi h} \right|^\gamma \hat{u}(\varpi), \end{aligned}$$

respectively, which further leads to

$$\Phi(\varpi, h) = |\varpi|^\gamma \left\{ -1 + \left[1 + \frac{\gamma}{6} \sin^2 \left(\frac{1}{2} \varpi h \right) + \frac{\gamma(5\gamma + 22)}{360} \sin^4 \left(\frac{1}{2} \varpi h \right) \right] \left| \frac{\sin \left(\frac{1}{2} \varpi h \right)}{\frac{1}{2} \varpi h} \right|^\gamma \right\} \hat{u}(\varpi).$$

From the Taylor expansions, there are

$$1 + \frac{\gamma}{6} \sin^2 \left(\frac{1}{2} \varpi h \right) + \frac{\gamma(5\gamma + 22)}{360} \sin^4 \left(\frac{1}{2} \varpi h \right) = 1 + \frac{\gamma}{24} (\varpi h)^2 + \frac{\gamma(5\gamma + 2)}{5760} (\varpi h)^4 + \mathcal{O}(\varpi h)^6,$$

and

$$\left| \frac{\sin \left(\frac{1}{2} \varpi h \right)}{\frac{1}{2} \varpi h} \right|^\gamma = 1 - \frac{\gamma}{24} (\varpi h)^2 + \frac{\gamma(5\gamma - 2)}{5760} (\varpi h)^4 + \mathcal{O}(\varpi h)^6,$$

we finally know that

$$\Phi(\varpi, h) = |\varpi|^\gamma \left[-\frac{\gamma^2}{34560} (\varpi h)^6 + \frac{\gamma^2(25\gamma^2 - 4)}{33177600} (\varpi h)^8 + \mathcal{O}(\varpi h)^{10} \right] \hat{u}(\varpi),$$

and there exist a positive constant C_1 , such that

$$(2.5) \quad |\Phi(\varpi, h)| \leq C_1 \left(|\varpi|^{\gamma+6} |\hat{u}(\varpi)| \right) h^6.$$

Using the inverse Fourier transform to equation (2.4), and combining with inequality (2.5) and condition $u(x) \in \mathcal{C}^{6+\gamma}(\mathbb{R})$, we can finally achieve the following result

$$\begin{aligned} \left| \partial_{x,\mathbb{R}}^\gamma u(x) - \delta_{h,\mathbb{R}}^\gamma u(x) \right| &= \left| \frac{1}{2\pi} \int_{\mathbb{R}} \Phi(\varpi, h) e^{i\varpi x} d\varpi \right| \leq \frac{1}{2\pi} \int_{\mathbb{R}} |\Phi(\varpi, h)| d\varpi \\ &\leq \frac{C_1}{2\pi} \left(\int_{\mathbb{R}} |\varpi|^{\gamma+6} |\hat{u}(\varpi)| d\varpi \right) h^6 \leq \frac{C_1}{2\pi} \left(\int_{\mathbb{R}} (1 + |\varpi|^{\gamma+6}) |\hat{u}(\varpi)| d\varpi \right) h^6 \\ &= C_2 h^6. \end{aligned}$$

Obviously, this is completely consistent with the result to be proved, which completes the proof. \square

Now, we consider the case for $x \in \Omega = [a, b] \subset \mathbb{R}$. If $u^*(x)$ is defined by

$$u^*(x) = \begin{cases} u(x), & x \in \Omega, \\ 0, & x \notin \Omega, \end{cases}$$

such that $u^*(x) \in \mathcal{C}^{6+\gamma}(\mathbb{R})$, then it follows from the Theorem 2.1 that $\partial_{x,\mathbb{R}}^\gamma u^*(x) = \delta_{h,\mathbb{R}}^\gamma u^*(x) + \mathcal{O}(h^6)$. Because of $u^*(x) = 0$ for $x \notin \Omega$, then we further obtain

$$(2.6) \quad \partial_{x,\Omega}^\gamma u(x) = \delta_{h,\Omega}^\gamma u(x) + \mathcal{O}(h^6),$$

where the operator $\delta_{h,\Omega}^\gamma$ is given by

$$(2.7) \quad \delta_{h,\Omega}^\gamma u(x) = -h^{-\gamma} \sum_{m=(x-b)/h}^{(x-a)/h} g_m^{(\gamma)} u(x - mh).$$

Let M be a positive integer, and $x_j = y_j = z_j = a + jh$, $j = 0, 1, \dots, M$, with $h = (b-a)/M$. Therefore, under homogeneous Dirichlet boundary conditions, it follows from equations (2.6) and (2.7), we can see that the discretization matrix of the operator \mathcal{L}^γ with mesh size h in one-dimensional is given by

$$\mathbf{D}_\gamma^{(1)} = -\frac{1}{h^\gamma} \mathbf{K}_\gamma,$$

with

$$\mathbf{K}_\gamma = \begin{pmatrix} g_0^{(\gamma)} & g_1^{(\gamma)} & g_2^{(\gamma)} & \cdots & g_{M-2}^{(\alpha)} \\ g_{-1}^{(\gamma)} & g_0^{(\gamma)} & g_1^{(\gamma)} & g_2^{(\gamma)} & \cdots \\ \vdots & \vdots & \ddots & \ddots & \ddots \\ g_{3-M}^{(\gamma)} & \cdots & g_{-1}^{(\alpha)} & g_0^{(\gamma)} & g_1^{(\gamma)} \\ g_{2-M}^{(\gamma)} & g_{3-M}^{(\gamma)} & \cdots & g_{-1}^{(\gamma)} & g_0^{(\gamma)} \end{pmatrix}_{(M-1) \times (M-1)}.$$

Similarly, it is easy to derive the corresponding discretization matrices of the operator \mathcal{L}^γ in two-dimensions and in three-dimensions are

$$\mathbf{D}_\gamma^{(2)} = -\frac{1}{h^\gamma} (\mathbf{I} \otimes \mathbf{K}_\gamma + \mathbf{K}_\gamma \otimes \mathbf{I}),$$

and

$$\mathbf{D}_\gamma^{(3)} = -\frac{1}{h^\gamma} (\mathbf{I} \otimes \mathbf{I} \otimes \mathbf{K}_\gamma + \mathbf{I} \otimes \mathbf{K}_\gamma \otimes \mathbf{I} + \mathbf{K}_\gamma \otimes \mathbf{I} \otimes \mathbf{I}),$$

respectively, where \mathbf{I} is an identity matrix of size $M - 1$ and the symbol \otimes represents the Kronecker product between the two matrices.

Once again, we study the properties of the coefficients $g_m^{(\gamma)} (m = 0, \pm 1, \pm 2, \dots)$. The main results are described in the following theorem.

LEMMA 2.2. *For the coefficients $g_m^{(\gamma)} (m = 0, \pm 1, \pm 2, \dots)$, the following properties hold:*

- (1) $g_0^{(\gamma)} \geq 0, g_{\pm 1}^{(\gamma)} \leq 0$;
- (2) $g_{\pm 2}^{(\gamma)} \leq 0$ if $\gamma \in (1, \gamma^*]$, while $g_{\pm 2}^{(\gamma)} \geq 0$ if $\gamma \in [\gamma^*, 2)$. Here, $\gamma^* = 1.4746120$;
- (3) $g_m^{(\gamma)} \leq 0, m = \pm 3, \pm 4, \dots$;
- (4) $\sum_{m=-\infty}^{+\infty} g_m^{(\gamma)} = 0$.

Proof. (1) From equation (2.3), we know that

$$g_0^{(\gamma)} = \frac{(\gamma + 2)(\gamma + 4)(5\gamma^4 + 102\gamma^3 + 763\gamma^2 + 2466\gamma + 2880)\Gamma(\gamma + 1)}{5760\Gamma^2(\gamma/2 + 3)} > 0,$$

and that

$$g_{\pm 1}^{(\gamma)} = -\frac{(5\gamma^4 + 122\gamma^3 + 1171\gamma^2 + 5278\gamma + 9624)\Gamma(\gamma + 1)}{90\gamma(\gamma + 2)(\gamma + 4)(\gamma + 6)\Gamma^2(\gamma/2)} < 0.$$

(2) In equation (2.3), we take $m = \pm 2$, and denote

$$(2.8) \quad g_{\pm 2}^{(\gamma)} = p_1(\gamma)q_1(\gamma),$$

where

$$(2.9) \quad p_1(\gamma) = 5\gamma^5 + 132\gamma^4 + 1415\gamma^3 + 6900\gamma^2 + 9380\gamma - 34032,$$

and

$$(2.10) \quad q_1(\gamma) = \frac{\Gamma(\gamma + 1)}{90\gamma(\gamma + 2)(\gamma + 4)(\gamma + 6)(\gamma + 8)\Gamma^2(\gamma/2)} > 0.$$

By Newton iteration method, we get a unique solution of the equation $p_1(\gamma) = 0$ for $\gamma \in (1, 2]$ is $\gamma^* = 1.474612$. Combining (2.8), (2.9) and (2.10), we can see that the conclusion is valid.

(3) Denote $g_m^{(\gamma)} = p_2(\gamma)[q_2(\gamma) + q_3(\gamma)]$, where

$$p_2(\gamma) = \frac{(-1)^m \Gamma(\gamma + 1)}{\Gamma(\gamma/2 - m + 1)\Gamma(\gamma/2 + m + 1)}, \quad q_2(\gamma) = 1 + \frac{\gamma(\gamma + 1)(\gamma + 2)}{6(\gamma - 2m + 2)(\gamma + 2m + 2)},$$

and

$$q_3(\gamma) = \frac{\gamma(\gamma + 1)(\gamma + 2)(\gamma + 3)(\gamma + 4)(5\gamma + 22)}{360(\gamma - 2m + 4)(\gamma - 2m + 2)(\gamma + 2m + 4)(\gamma + 2m + 2)}.$$

From [8], we know that $p_2(\gamma) \leq 0$ for all $|m| \geq 1$ and $\gamma \in (1, 2]$. Meanwhile, for $\gamma \in (1, 2]$ and all $|m| \geq 3$, there also holds that

$$\begin{aligned} q_2(\gamma) &= 1 + \frac{\gamma(\gamma + 1)(\gamma + 2)}{6(\gamma - 2m + 2)(\gamma + 2m + 2)} \geq \left[1 + \frac{\gamma(\gamma + 1)(\gamma + 2)}{6(\gamma - 2m + 2)(\gamma + 2m + 2)} \right] \Big|_{m=\pm 3} \\ &= \frac{144 - \gamma(\gamma^2 + 9\gamma + 14)}{6(\gamma + 6)(4 - \gamma)} > 0, \quad 7 \end{aligned}$$

and

$$q_3(\gamma) > \frac{\gamma(\gamma+1)(\gamma+2)(\gamma+3)(\gamma+4)(5\gamma+22)}{360} \left(\frac{1}{2m}\right)^4 > 0.$$

This shows that $g_m^{(\gamma)} = p_2(\gamma) [q_2(\gamma) + q_3(\gamma)] \leq 0$ for all $|m| \geq 3$ and $\gamma \in (1, 2]$.

(4) By taking $w = 1$ in equation (2.2) and combining it with equation (2.1), the result to be proved can be obtained immediately, which completes all the proofs. \square

After studying the high-order numerical differential formula of Riesz derivative and its corresponding coefficients, we immediately turn to consider the equation (1.1). Denote

$$\mathbf{u}(\mathbf{x}, t) = [u(\mathbf{x}_1, t), u(\mathbf{x}_2, t), \dots, u(\mathbf{x}_{M-1}, t)]^\top$$

as the solution vector of (1.1) on the spatial mesh, using the numerical differential formula (2.6) to the equation (1.1), then we obtain the corresponding semi-discrete scheme as follows

$$(2.11) \quad \frac{d\mathbf{u}(\mathbf{x}, t)}{dt} + \mathbf{A}^{(d)}\mathbf{u}(\mathbf{x}, t) = \mathbf{f}(\mathbf{u}) + R_h, \quad d = 1, 2, 3,$$

where $\mathbf{A}^{(d)} = -\epsilon^2 \mathbf{D}_\gamma^{(d)}$, and R_h is the local truncation error in spatial direction. Meanwhile, it follows from the numerical differential formula (2.6), there holds that

$$(2.12) \quad \|R_h\|_\infty \leq C_3 h^6$$

as the exact solution $\mathbf{u}(\mathbf{x}, \cdot) \in \mathcal{C}^{6+\gamma}(\overline{\Omega})$, where C_3 is a positive constant depending on the exact solution $\mathbf{u}(\mathbf{x}, t)$ but not depending on h .

2.2. Time discretization. For the time discretization, let us consider a uniform partition of the time interval $[0, T] : 0 = t_0 < t_1 < \dots < t_N = T$, with the step size $\tau = T/N$. Using implicit integration factor method [23], the exact solution of the equation (2.11) is given by the following equation

$$\mathbf{u}(\mathbf{x}, t) = e^{-t\mathbf{A}^{(d)}} \mathbf{u}_0 + \int_0^t e^{-(t-s)\mathbf{A}^{(d)}} \mathbf{f}(\mathbf{u}(\mathbf{x}, s)) ds + \tau R_h,$$

which satisfies the recurrence formula

$$(2.13) \quad \mathbf{u}(\mathbf{x}, t_{k+1}) = e^{-\tau\mathbf{A}^{(d)}} \mathbf{u}(\mathbf{x}, t_k) + \int_0^\tau e^{-(\tau-s)\mathbf{A}^{(d)}} \mathbf{f}(\mathbf{u}(\mathbf{x}, t_k + s)) ds + \tau R_h.$$

By using the [1,1] padé approximation [24] to deal with the exponential matrices and the trapezoidal method to compute the resulting integral in equation (2.13), we obtain the following equation

$$(2.14) \quad \begin{aligned} \mathbf{u}(\mathbf{x}, t_{k+1}) &= \left(\mathbf{I} + \frac{\tau}{2}\mathbf{A}^{(d)}\right)^{-1} \left(\mathbf{I} - \frac{\tau}{2}\mathbf{A}^{(d)}\right) \mathbf{u}(\mathbf{x}, t_k) \\ &\quad + \int_0^\tau \left(\mathbf{I} + \frac{\tau-s}{2}\mathbf{A}^{(d)}\right)^{-1} \left(\mathbf{I} - \frac{\tau-s}{2}\mathbf{A}^{(d)}\right) \mathbf{f}(\mathbf{u}(\mathbf{x}, t_k + s)) ds \\ &\quad + \tau(R_\tau + R_h) \\ &= \left(\mathbf{I} + \frac{\tau}{2}\mathbf{A}^{(d)}\right)^{-1} \left(\mathbf{I} - \frac{\tau}{2}\mathbf{A}^{(d)}\right) \mathbf{u}(\mathbf{x}, t_k) \\ &\quad + \frac{\tau}{2}\mathbf{f}(\mathbf{u}(\mathbf{x}, t_{k+1})) + \frac{\tau}{2} \left(\mathbf{I} + \frac{\tau}{2}\mathbf{A}^{(d)}\right)^{-1} \left(\mathbf{I} - \frac{\tau}{2}\mathbf{A}^{(d)}\right) \mathbf{f}(\mathbf{u}(\mathbf{x}, t_k)) \\ &\quad + \tau(R_\tau + R_h), \end{aligned}$$

where R_τ is the local truncation error in temporal direction and satisfies

$$(2.15) \quad \|R_\tau\|_\infty \leq C_4 \tau^2$$

for $\mathbf{u}(\cdot, t) \in C^2[0, T]$, where C_4 is also a positive constant that depends on the exact solution $\mathbf{u}(\mathbf{x}, t)$ rather than τ .

Omitting the truncation error $\tau(R_\tau + R_h)$ in the above equation, and replacing exact solution $\mathbf{u}(\mathbf{x}, t_k)$ by its numerical solution \mathbf{U}^k , then we can obtain a high-order difference scheme for equation (1.1) as follows

$$(2.16) \quad \begin{aligned} \mathbf{U}^{k+1} &= \left(\mathbf{I} + \frac{\tau}{2} \mathbf{A}^{(d)}\right)^{-1} \left(\mathbf{I} - \frac{\tau}{2} \mathbf{A}^{(d)}\right) \mathbf{U}^k + \frac{\tau}{2} \mathbf{f}(\mathbf{U}^{k+1}) \\ &+ \frac{\tau}{2} \left(\mathbf{I} + \frac{\tau}{2} \mathbf{A}^{(d)}\right)^{-1} \left(\mathbf{I} - \frac{\tau}{2} \mathbf{A}^{(d)}\right) \mathbf{f}(\mathbf{U}^k), \quad k = 0, 1, \dots, N-1. \end{aligned}$$

3. Theoretical analysis of the numerical scheme. In this section, for simplicity, we only consider the one dimensional space fractional Allen-Cahn equation, i.e., $d = 1$. From equation (2.16), it is not difficult to obtain the corresponding numerical scheme for case $d = 1$ as follows

$$(3.1) \quad \begin{aligned} \mathbf{U}^{k+1} &= \left(\mathbf{I} + \frac{\tau}{2} \mathbf{A}^{(1)}\right)^{-1} \left(\mathbf{I} - \frac{\tau}{2} \mathbf{A}^{(1)}\right) \mathbf{U}^k + \frac{\tau}{2} \mathbf{f}(\mathbf{U}^{k+1}) \\ &+ \frac{\tau}{2} \left(\mathbf{I} + \frac{\tau}{2} \mathbf{A}^{(1)}\right)^{-1} \left(\mathbf{I} - \frac{\tau}{2} \mathbf{A}^{(1)}\right) \mathbf{f}(\mathbf{U}^k), \quad k = 0, 1, \dots, N-1. \end{aligned}$$

3.1. Preliminaries. For the convenience of subsequent analysis, we list some basic symbols and related lemmas in this section. First, define the following space

$$\dot{\Psi}_h = \{\mathbf{U} : \mathbf{U} = \{U_j\} \text{ is grid function and } U_0 = U_M = 0\},$$

equipped with discrete inner product and the associated L^2 norm defined as

$$\langle \mathbf{U}, \mathbf{V} \rangle := h \mathbf{V}^T \mathbf{U} = h \sum_{j=1}^{M-1} U_j V_j, \quad \|\mathbf{U}\|_2 = \sqrt{\langle \mathbf{U}, \mathbf{U} \rangle}, \quad \text{for any } \mathbf{U}, \mathbf{V} \in \dot{\Psi}_h.$$

Besides, we can also give the following discrete L^∞ norm

$$\|\mathbf{U}\|_\infty = \max_{1 \leq j \leq M-1} |U_j|.$$

DEFINITION 3.1. (See [25]) Let $n \times n$ Toeplitz matrix \mathbf{Q}_n be in the form:

$$\mathbf{Q}_n = \begin{pmatrix} q_0 & q_{-1} & \cdots & q_{2-n} & q_{1-n} \\ q_1 & q_0 & q_{-1} & \cdots & q_{2-n} \\ \vdots & q_1 & q_0 & \ddots & \vdots \\ q_{n-2} & \cdots & \ddots & \ddots & q_{-1} \\ q_{n-1} & q_{n-2} & \cdots & q_1 & q_0 \end{pmatrix},$$

i.e., $q_{ij} = q_{i-j}$. Assume that the diagonals are the Fourier coefficients of the function f , i.e.,

$$q_k = \frac{1}{2\pi} \int_{-\pi}^{\pi} f(x) e^{-ikx} dx,$$

then function $f(x)$ is called the generating function of \mathbf{Q}_n .

LEMMA 3.2. (*Grenander-Szegö Theorem [26]*) For the above Toeplitz matrix \mathbf{Q}_n , let $f(x)$ be a 2π -periodic continuous real-valued function defined on $[-\pi, \pi]$. Denote $\lambda_{\min}(\mathbf{Q}_n)$ and $\lambda_{\max}(\mathbf{Q}_n)$ as the smallest and largest eigenvalues of \mathbf{Q}_n , respectively. Then one has

$$f_{\min} \leq \lambda_{\min}(\mathbf{Q}_n) \leq \lambda_{\max}(\mathbf{Q}_n) \leq f_{\max},$$

where f_{\min} , f_{\max} are the minimum and maximum values of $f(x)$ on $[-\pi, \pi]$. Moreover, if $f_{\min} < f_{\max}$, then all eigenvalues of \mathbf{Q}_n satisfy

$$f_{\min} < \lambda(\mathbf{Q}_n) < f_{\max},$$

for all $n > 0$.

LEMMA 3.3. The matrix \mathbf{K}_γ has the following properties:

- (1) \mathbf{K}_γ is symmetric;
- (2) \mathbf{K}_γ is positive definite, i.e., $\mathbf{W}^\top \mathbf{K}_\gamma \mathbf{W} > 0$ for any nonzero $\mathbf{W} \in \mathbb{R}^{M-1}$.

Proof. (1) From the equation (2.3), we can easily find that $g_m^{(\gamma)} = g_{-m}^{(\gamma)}$, which shows that the matrix \mathbf{K}_γ is symmetric.

(2) Based on the Definition 3.1 and the equation (2.2), we can know the generating function of the matrix \mathbf{K}_γ is

$$\begin{aligned} g(\gamma, z) &= \sum_{m=-\infty}^{+\infty} g_m^{(\gamma)} e^{imz} \\ &= \left[1 + \frac{\gamma}{24} (2 - e^{iz} - e^{-iz}) + \frac{\gamma(5\gamma + 22)}{5760} (2 - e^{iz} - e^{-iz})^2 \right] (2 - e^{iz} - e^{-iz})^{\frac{\gamma}{2}} \\ &= \left[1 + \frac{\gamma}{6} \sin^2\left(\frac{z}{2}\right) + \frac{\gamma(5\gamma + 22)}{360} \sin^4\left(\frac{z}{2}\right) \right] \left[4 \sin^2\left(\frac{z}{2}\right) \right]^{\frac{\gamma}{2}} \geq 0 \end{aligned}$$

for $z \in [-\pi, \pi]$ and $\gamma \in (1, 2]$. This implies that matrix \mathbf{K}_γ is positive definite for $1 < \gamma \leq 2$ based on Lemma 3.2. \square

LEMMA 3.4. There exist real symmetric positive matrix $\mathbf{L}^{(1)}$ such that the following inner product equality holds:

$$(\mathbf{A}^{(1)} \mathbf{U}, \mathbf{V}) = (\mathbf{L}^{(1)} \mathbf{U}, \mathbf{L}^{(1)} \mathbf{V}).$$

Proof. From the Lemma 3.3, we know that the matrix $\mathbf{A}^{(1)}$ is a real positive definite symmetric matrix. Hence, based on the basic properties of matrix, there is a real orthogonal matrix \mathbf{P} and a real diagonal matrix $\mathbf{\Lambda} = \text{diag}(\lambda)$, such that

$$(3.2) \quad \mathbf{A}^{(1)} = \mathbf{P} \mathbf{\Lambda} \mathbf{P}^\top = (\mathbf{P} \mathbf{\Lambda}^{\frac{1}{2}} \mathbf{P}^\top)^\top (\mathbf{P} \mathbf{\Lambda}^{\frac{1}{2}} \mathbf{P}^\top) = (\mathbf{L}^{(1)})^\top \mathbf{L}^{(1)},$$

where $\mathbf{\Lambda}^{\frac{1}{2}} = \text{diag}(\lambda^{\frac{1}{2}})$ and $\mathbf{L}^{(1)} = \mathbf{P} \mathbf{\Lambda}^{\frac{1}{2}} \mathbf{P}^\top$. Furthermore, with the help of the decomposition (3.2), one has

$$(\mathbf{A}^{(1)} \mathbf{U}, \mathbf{V}) = \mathbf{V}^\top \mathbf{A}^{(1)} \mathbf{U} = \mathbf{V}^\top (\mathbf{L}^{(1)})^\top \mathbf{L}^{(1)} \mathbf{U} = (\mathbf{L}^{(1)} \mathbf{V})^\top \mathbf{L}^{(1)} \mathbf{U} = (\mathbf{L}^{(1)} \mathbf{U}, \mathbf{L}^{(1)} \mathbf{V}).$$

This completes the proof. \square

LEMMA 3.5. (*Brouwer fixed point theorem [29]*) Let $(H, \langle \cdot, \cdot \rangle)$ be a finite-dimensional inner product space, $\|\cdot\|$ be the associated norm, and $\mathcal{H} : H \rightarrow H$ be continuous. Assume, moreover, that

$$\exists \sigma > 0, \forall z \in H, \|z\| = \sigma, \Re \langle \mathcal{H}(z), z \rangle > 0.$$

Then, there exists a $z^* \in H$ such that $\mathcal{G}(z^*) = 0$ and $\|z^*\| \leq \sigma$.

LEMMA 3.6. Let $\mathbf{A}^{(1)}$ be a real $(M-1) \times (M-1)$ matrix and satisfy the conditions of Lemma 3.3, then we have

$$\left\| \left(\mathbf{I} + \frac{\tau}{2} \mathbf{A}^{(1)} \right)^{-1} \left(\mathbf{I} - \frac{\tau}{2} \mathbf{A}^{(1)} \right) \right\|_{\infty} < 1$$

for any $\tau > 0$.

Proof. Let $\lambda_j(\mathbf{A}^{(1)})$, $j = 1, 2, \dots, M-1$ be the eigenvalues of matrix $\mathbf{A}^{(1)}$ and denote $\mathbf{B} = \left(\mathbf{I} + \frac{\tau}{2} \mathbf{A}^{(1)} \right)^{-1} \left(\mathbf{I} - \frac{\tau}{2} \mathbf{A}^{(1)} \right)$, then the eigenvalues of the matrix \mathbf{B} are

$$\lambda_j(\mathbf{B}) = \frac{1 - \frac{\tau}{2} \lambda_j(\mathbf{A}^{(1)})}{1 + \frac{\tau}{2} \lambda_j(\mathbf{A}^{(1)})}, \quad j = 1, 2, \dots, M-1.$$

The matrix $\mathbf{A}^{(1)}$ satisfies the conditions of Lemma 3.3, which imply that $\lambda_j(\mathbf{A}^{(1)}) > 0$, and it is not hard to check that $|\lambda_j(\mathbf{B})| < 1$ for any $\tau > 0$. Therefore, this reflects that the spectral radius of the matrix \mathbf{B} is less than 1, so the result to be proved is valid. \square

LEMMA 3.7. Let $g(x) = x + \frac{\tau}{2} f(x)$ with $f(x) = x - x^3$. Then there holds that

$$|g(x)| \leq 1 \text{ for all } x \in [-1, 1] \text{ and } \tau \in (0, 1].$$

Proof. Due to $g'(x) = 1 + \frac{\tau}{2} f'(x) \geq 0$ for all $x \in [-1, 1]$ and $\tau \in (0, 1]$, then we know that $g(-1) \leq g(x) \leq g(1)$. Moreover, note that $g(-1) = -1$ and $g(1) = 1$, then we deduce that

$$-1 \leq g(x) \leq 1 \text{ for all } x \in [-1, 1],$$

which concludes the proof. \square

LEMMA 3.8. Let $\lambda_j(\mathbf{A}^{(1)})$, $j = 1, 2, \dots, M-1$, be the eigenvalue of the matrix $\mathbf{A}^{(1)}$. Then there holds that

$$\lambda_j(\mathbf{A}^{(1)}) \leq \begin{cases} \frac{2\varepsilon^2}{h^\gamma} g_0^{(\gamma)}, & \gamma \in (1, \gamma^*]; \\ \frac{2\varepsilon^2}{h^\gamma} (g_0^{(\gamma)} + 2g_2^{(\gamma)}), & \gamma \in (\gamma^*, 2], \end{cases} \quad j = 1, 2, \dots, M-1.$$

Proof. From the Gerschgorin's circle theorem [27], we know that

$$\left| \lambda_j(\mathbf{A}^{(1)}) - \frac{\varepsilon^2}{h^\gamma} g_0^{(\gamma)} \right| \leq \frac{\varepsilon^2}{h^\gamma} \sum_{\substack{m=-M+j \\ m \neq 0}}^{j-1} |g_m^{(\gamma)}| = \frac{\varepsilon^2}{h^\gamma} \sum_{m=-M+j}^{j-1} |g_m^{(\gamma)}| - \frac{\varepsilon^2}{h^\gamma} g_0^{(\gamma)}, \quad j = 1, 2, \dots, M-1,$$

that is

$$(3.3) \quad \lambda_j(\mathbf{A}^{(1)}) \leq \frac{\varepsilon^2}{h^\gamma} \sum_{m=-M+j}^{j-1} |g_m^{(\gamma)}| \leq \frac{\varepsilon^2}{h^\gamma} \sum_{m=-\infty}^{+\infty} |g_m^{(\gamma)}| := \frac{\varepsilon^2}{h^\gamma} S_m.$$

It follows from the Lemma 2.2, one has

$$(3.4) \quad S_m = \sum_{m=-\infty}^{-1} |g_m^{(\gamma)}| + |g_0^{(\gamma)}| + \sum_{m=1}^{+\infty} |g_m^{(\gamma)}| = - \sum_{m=-\infty}^{-1} g_m^{(\gamma)} + g_0^{(\gamma)} - \sum_{m=1}^{+\infty} g_m^{(\gamma)} = 2g_0^{(\gamma)}$$

for $\gamma \in (1, \gamma^*]$, and

$$(3.5) \quad S_m = - \sum_{m=-\infty}^{-3} g_m^{(\gamma)} + g_{-2}^{(\gamma)} - g_{-1}^{(\gamma)} + g_0^{(\gamma)} - g_1^{(\gamma)} + g_2^{(\gamma)} - \sum_{m=3}^{+\infty} g_m^{(\gamma)} = 2(g_0^{(\gamma)} + 2g_2^{(\gamma)})$$

for $\gamma \in (\gamma^*, 2]$. Combining (3.3), (3.4) and (3.5), we can easily know that the conclusion to be proved is valid. This completes the proof. \square

LEMMA 3.9. (*Gronwall inequality*[28]). Suppose $\{E^k\}_{k=0}^{\infty}$ is a nonnegative sequence and satisfies

$$E^{k+1} \leq (1 + c\tau) E^k + \tau g, \quad k = 0, 1, \dots$$

Then we have

$$E^k \leq \exp(ck\tau) \left(E^0 + \frac{g}{c} \right), \quad k = 1, 2, \dots,$$

where c and g are nonnegative constants.

3.2. Unique solvability. In this section, the uniquely solvability of the finite difference scheme (3.1) will be given by the following theorems.

THEOREM 3.10. *The solution of the finite difference scheme (3.1) exists.*

Proof. Denote $\Theta = \mathbf{U}^{k+\frac{1}{2}}$. For a fixed k , the difference scheme (3.1) can be rewritten as

$$(3.6) \quad \begin{aligned} \Theta = & \frac{2}{2-\tau} \left\{ \mathbf{U}^k - \frac{\tau}{2} \mathbf{A}^{(1)} \Theta - \frac{\tau}{4} \left[(\mathbf{U}^k)^3 + (2\Theta - \mathbf{U}^k)^3 \right] \right. \\ & \left. + \frac{\tau^2}{4} \mathbf{A}^{(1)} (\Theta - \mathbf{U}^k) + \frac{\tau^2}{8} \mathbf{A}^{(1)} \left[(\mathbf{U}^k)^3 - (2\Theta - \mathbf{U}^k)^3 \right] \right\}. \end{aligned}$$

Based on the equation (3.6), let us define a mapping $\mathcal{H} : \Psi_h \rightarrow \Psi_h$ as follows

$$\begin{aligned} \mathcal{H}(\Theta) = & \Theta - \frac{2}{2-\tau} \left\{ \mathbf{U}^k - \frac{\tau}{2} \mathbf{A}^{(1)} \Theta - \frac{\tau}{4} \left[(\mathbf{U}^k)^3 + (2\Theta - \mathbf{U}^k)^3 \right] \right. \\ & \left. + \frac{\tau^2}{4} \mathbf{A}^{(1)} (\Theta - \mathbf{U}^k) + \frac{\tau^2}{8} \mathbf{A}^{(1)} \left[(\mathbf{U}^k)^3 - (2\Theta - \mathbf{U}^k)^3 \right] \right\}, \end{aligned}$$

which is obviously continuous. Taking the inner product of above equation with Θ and using Lemma 3.4, there is

$$\begin{aligned} \langle \mathcal{H}(\Theta), \Theta \rangle &= \langle \Theta, \Theta \rangle - \frac{2}{2-\tau} \left\{ \langle \mathbf{U}^k, \Theta \rangle - \frac{\tau}{2} \langle \mathbf{A}^{(1)} \Theta, \Theta \rangle - \frac{\tau}{4} \langle (\mathbf{U}^k)^3 + (2\Theta - \mathbf{U}^k)^3, \Theta \rangle \right. \\ & \quad \left. + \frac{\tau^2}{4} \langle \mathbf{A}^{(1)} (\Theta - \mathbf{U}^k), \Theta \rangle + \frac{\tau^2}{8} \langle \mathbf{A}^{(1)} \left[(\mathbf{U}^k)^3 - (2\Theta - \mathbf{U}^k)^3 \right], \Theta \rangle \right\} \\ &= \|\Theta\|^2 - \frac{2}{2-\tau} \langle \mathbf{U}^k, \Theta \rangle + \frac{\tau}{2-\tau} \|\mathbf{L}^{(1)} \Theta\|^2 + \frac{4\tau}{2-\tau} \|\Theta\|^4 - \frac{6\tau}{2-\tau} \langle \Theta^2 \mathbf{U}^k, \Theta \rangle \\ & \quad + \frac{3\tau}{2-\tau} \|\Theta \mathbf{U}^k\|^2 - \frac{\tau^2}{2(2-\tau)} \|\mathbf{L}^{(1)} \Theta\|^2 + \frac{\tau^2}{2(2-\tau)} \langle \mathbf{L}^{(1)} \mathbf{U}^k, \mathbf{L}^{(1)} \Theta \rangle \\ & \quad - \frac{\tau^2}{2(2-\tau)} \langle \mathbf{L}^{(1)} (\mathbf{U}^k)^3, \mathbf{L}^{(1)} \Theta \rangle + \frac{2\tau^2}{2-\tau} \langle \mathbf{L}^{(1)} \Theta^3, \mathbf{L}^{(1)} \Theta \rangle \\ & \quad - \frac{3\tau^2}{2-\tau} \langle \mathbf{L}^{(1)} \Theta^2 \mathbf{U}^k, \mathbf{L}^{(1)} \Theta \rangle + \frac{3\tau^2}{2(2-\tau)} \langle \mathbf{L}^{(1)} \Theta (\mathbf{U}^k)^2, \mathbf{L}^{(1)} \Theta \rangle. \end{aligned}$$

Furthermore, by using the Cauchy-Schwarz inequality, we can obtain

$$\begin{aligned} \langle \mathcal{H}(\Theta), \Theta \rangle \geq & \|\Theta\| \left[\|\Theta\| - \frac{2}{2-\tau} \|\mathbf{U}^k\| - \frac{6\tau}{2-\tau} \|\mathbf{U}^k\| \|\Theta\|^2 - \frac{\tau^2}{2(2-\tau)} \|\mathbf{L}^{(1)}\|^2 \|\mathbf{U}^k\| \right. \\ & \left. - \frac{\tau^2}{2(2-\tau)} \|\mathbf{L}^{(1)}\|^2 \|\mathbf{U}^k\|^3 - \frac{3\tau^2}{2-\tau} \|\mathbf{L}^{(1)}\|^2 \|\mathbf{U}^k\| \|\Theta\|^2 \right] \end{aligned}$$

under the condition of $0 < \tau < 2$.

Let

$$\Delta = \tilde{\tau}^2 - 6\tau \|\mathbf{U}^k\| (2 + \tau \lambda_{\max}(\mathbf{A}^{(1)})) \left\{ 2\tilde{\tau} + \|\mathbf{U}^k\| \left[4 + \tau^2 \lambda_{\max}(\mathbf{A}^{(1)}) (1 + \|\mathbf{U}^k\|^2) \right] \right\} \geq 0,$$

and

$$\mu = \frac{\tilde{\tau} + \sqrt{\Delta}}{6\tau \|\mathbf{U}^k\| (2 + \tau \lambda_{\max}(\mathbf{A}^{(1)}))},$$

where $\tilde{\tau} = 2 - \tau$, then we obtain $\langle \mathcal{H}(\Theta), \Theta \rangle \geq \|\Theta\| \geq 0$, when $\|\Theta\| = \mu$. Thus, there exists a solution $\mu^* \in \dot{\Psi}_h$ satisfying $\mathcal{H}(\mu^*) = 0$. Hence, we can draw a conclusion that the difference scheme (3.1) exists solution by follows form the Lemma 3.5. This completes the proof. \square

For technical needs, the uniqueness of the solution will be considered after the Discrete maximum principle is proved.

3.3. Discrete maximum principle. In this section, we will show that the difference scheme (3.1) preserves the discrete maximum principle.

THEOREM 3.11. *Suppose that the initial condition $u_0(x)$ satisfies $\max_{x \in \bar{\Omega}} |u_0(x)| \leq 1$, if the time step τ satisfies*

$$(3.7) \quad 0 < \tau \leq 1,$$

then the numerical solution $\{\mathbf{U}^{k+1}\}$ generated by the difference scheme (3.1) also satisfies the discrete maximum bound principle, i.e.,

$$\|\mathbf{U}^{k+1}\|_{\infty} \leq 1, \quad k = 0, 1, \dots, N-1.$$

Proof. Here, we use mathematical induction method to prove it. For the case of $k = 0$, it is clearly true. Suppose that $\|\mathbf{U}^n\|_{\infty} \leq 1$ is true for $n = 1, 2, \dots, k$. Next, we will prove that $\|\mathbf{U}^{k+1}\|_{\infty} \leq 1$ is also true. From scheme (3.1), we can see that

$$(3.8) \quad \left\| \mathbf{U}^{k+1} - \frac{\tau}{2} \mathbf{f}(\mathbf{U}^{k+1}) \right\|_{\infty} = \left\| \mathbf{B} \left(\mathbf{U}^k + \frac{\tau}{2} \mathbf{f}(\mathbf{U}^k) \right) \right\|_{\infty},$$

where $\mathbf{B} = \left(\mathbf{I} + \frac{\tau}{2} \mathbf{A}^{(1)} \right)^{-1} \left(\mathbf{I} - \frac{\tau}{2} \mathbf{A}^{(1)} \right)$.

Obviously, the left-hand side of equation (3.8) becomes

$$(3.9) \quad \left\| \mathbf{U}^{k+1} - \frac{\tau}{2} \mathbf{f}(\mathbf{U}^{k+1}) \right\|_{\infty} = \left(1 - \frac{\tau}{2} \right) \|\mathbf{U}^{k+1}\|_{\infty} + \frac{\tau}{2} \|\mathbf{U}^{k+1}\|_{\infty}^3$$

for $0 < \tau \leq 2$.

Under the condition of (3.7), using Lemmas 3.6 and 3.7, and note that $\|\mathbf{U}^k\|_{\infty} \leq 1$, we know that the right-hand side of equation (3.8) satisfies

$$(3.10) \quad \left\| \mathbf{B} \left(\mathbf{U}^k + \frac{\tau}{2} \mathbf{f}(\mathbf{U}^k) \right) \right\|_{\infty} \leq \|\mathbf{B}\|_{\infty} \left\| \mathbf{U}^k + \frac{\tau}{2} \mathbf{f}(\mathbf{U}^k) \right\|_{\infty} \leq 1.$$

Combining (3.8), (3.9) and (3.10) can lead to

$$\left(1 - \frac{\tau}{2}\right) \|\mathbf{U}^{k+1}\|_\infty + \frac{\tau}{2} \|\mathbf{U}^{k+1}\|_\infty^3 \leq 1,$$

that is

$$\left(\|\mathbf{U}^{k+1}\|_\infty - 1\right) \left(\|\mathbf{U}^{k+1}\|_\infty^2 + \|\mathbf{U}^{k+1}\|_\infty + \frac{2}{\tau}\right) \leq 0,$$

which implies that $\|\mathbf{U}^{k+1}\|_\infty \leq 1$. This completes the proof. \square

THEOREM 3.12. *The solution of the finite difference scheme (3.1) is unique.*

Proof. Let \mathbf{U}^k and \mathbf{V}^k be the numerical solutions of the scheme (3.1) and denote

$$\xi^k = \mathbf{U}^k - \mathbf{V}^k, \quad k = 0, 1, \dots, N.$$

Based on difference scheme (3.1), it is not difficult to find that ξ^k satisfies the following equation

$$(3.11) \quad \left[\left(1 - \frac{\tau}{2}\right)\mathbf{I} + \frac{\tau}{2}\mathbf{A}^{(1)}\right] \xi^{k+1} = \left[\left(1 + \frac{\tau}{2}\right)\mathbf{I} - \frac{\tau}{2}\mathbf{A}^{(1)}\right] \xi^k + \alpha^{k+1/2}, \quad k = 0, 1, \dots, N-1,$$

where

$$\alpha^{k+1/2} = \frac{\tau}{2} \left[(\mathbf{V}^{k+1})^3 - (\mathbf{U}^{k+1})^3 \right] + \frac{\tau}{2} \left(\mathbf{I} - \frac{\tau}{2} \mathbf{A}^{(1)} \right) \left[(\mathbf{V}^k)^3 - (\mathbf{U}^k)^3 \right].$$

Computing the discrete inner product of (3.11) with $2\xi^{k+1/2}$ yield

$$(3.12) \quad \begin{aligned} & \left\langle \left[\left(1 - \frac{\tau}{2}\right)\mathbf{I} + \frac{\tau}{2}\mathbf{A}^{(1)}\right] \xi^{k+1}, 2\xi^{k+1/2} \right\rangle - \left\langle \left[\left(1 + \frac{\tau}{2}\right)\mathbf{I} - \frac{\tau}{2}\mathbf{A}^{(1)}\right] \xi^k, 2\xi^{k+1/2} \right\rangle \\ & = \left\langle \alpha^{k+1/2}, 2\xi^{k+1/2} \right\rangle. \end{aligned}$$

Next, we will proceed to analyze each term in equation (3.12). Firstly, for the left-hand term of equation (3.12), with the help of Lemma 3.4 and Cauchy-Schwarz inequality, we can see that

$$(3.13) \quad \begin{aligned} & \left\langle \left[\left(1 - \frac{\tau}{2}\right)\mathbf{I} + \frac{\tau}{2}\mathbf{A}^{(1)}\right] \xi^{k+1}, 2\xi^{k+1/2} \right\rangle - \left\langle \left[\left(1 + \frac{\tau}{2}\right)\mathbf{I} - \frac{\tau}{2}\mathbf{A}^{(1)}\right] \xi^k, 2\xi^{k+1/2} \right\rangle \\ & \geq (1 - \tau) \|\xi^{k+1}\|^2 - (1 + \tau) \|\xi^k\|^2. \end{aligned}$$

For the right-hand term of equation (3.12), it holds that

$$(3.14) \quad \begin{aligned} \left\langle \alpha^{k+1/2}, 2\xi^{k+1/2} \right\rangle & = \frac{\tau}{2} \left\langle \left[(\mathbf{V}^{k+1})^3 - (\mathbf{U}^{k+1})^3 \right], 2\xi^{k+1/2} \right\rangle \\ & \quad + \frac{\tau}{2} \left\langle \left(\mathbf{I} - \frac{\tau}{2} \mathbf{A}^{(1)} \right) \left[(\mathbf{V}^k)^3 - (\mathbf{U}^k)^3 \right], 2\xi^{k+1/2} \right\rangle \\ & = \Xi_1 + \Xi_2. \end{aligned}$$

Next, we will analyze Ξ_1 and Ξ_2 . For Ξ_1 , it follows from the Cauchy-Schwarz inequality, we can know that

$$(3.15) \quad \Xi_1 = \frac{\tau}{2} \left\langle \left[(\mathbf{V}^{k+1})^3 - (\mathbf{U}^{k+1})^3 \right], 2\xi^{k+1/2} \right\rangle \leq \frac{3\tau}{4} \hat{C}_{\max}^2 \left(3 \|\xi^{k+1}\|^2 + \|\xi^k\|^2 \right),$$

where $\hat{C}_{\max} = \max\{\|\mathbf{U}^{k+1}\|, \|\mathbf{V}^{k+1}\|\}$. Similarly, for Ξ_2 , we also have

$$(3.16) \quad \Xi_2 \leq \frac{3\tau}{8} \tilde{C}_{\max}^2 (2 + \tau \|\mathbf{A}^{(1)}\|) (3 \|\xi^k\|^2 + \|\xi^{k+1}\|^2),$$

where $\tilde{C}_{\max} = \max\{\|\mathbf{U}^k\|, \|\mathbf{V}^k\|\}$.

Combining (3.14), (3.15) and (3.16), we can conclude that

$$(3.17) \quad \langle a^{k+1/2}, 2\xi^{k+1/2} \rangle \leq 4\tau C_{\max} (\|\xi^k\|^2 + \|\xi^{k+1}\|^2),$$

where $C_{\max} = \left\{ \frac{3}{4} \hat{C}_{\max}^2, \frac{3}{8} \tilde{C}_{\max}^2 \right\}$.

Substituting (3.13) and (3.17) into (3.12), and when $\tau(4C_{\max} + 1) \leq 1/2$, it can eventually lead to

$$\|\xi^k\| \leq 3^{N/2} \|\xi^0\| = 0, \quad k = 0, 1, 2, \dots, N,$$

due to $\|\xi^0\| = 0$, which implies that $\mathbf{U}^k = \mathbf{V}^k$. The proof is complete. \square

3.4. Discrete energy stability. First, we define the following discrete energy function

$$(3.18) \quad \mathcal{E}_h(\mathbf{U}) = \langle F(\mathbf{U}), \mathbf{1} \rangle + \frac{h}{2} \mathbf{U}^T \mathbf{A}^{(1)} \mathbf{U},$$

for all $\mathbf{U} = [U_1, U_2, \dots, U_{M-1}]^T \in \mathbb{R}^{M-1}$ and $\mathbf{1} = [1, 1, \dots, 1]^T \in \mathbb{R}^{M-1}$. Here, we will prove the energy stability of numerical scheme (3.1), that is, we will prove that the energy function $\mathcal{E}_h(\mathbf{U})$ decreases with time.

THEOREM 3.13. *Under the assumption of*

$$(3.19) \quad 0 < \tau \leq \begin{cases} \frac{4}{1 + \sqrt{1 + \frac{16\varepsilon^2}{h^\gamma} g_0^{(\gamma)}}}, & \gamma \in (1, \gamma^*]; \\ \frac{4}{1 + \sqrt{1 + \frac{16\varepsilon^2}{h^\gamma} (g_0^{(\gamma)} + 2g_2^{(\gamma)})}}, & \gamma \in (\gamma^*, 2], \end{cases}$$

the solution generated by the difference method (3.1) satisfies the energy stability, i.e.,

$$\mathcal{E}_h(\mathbf{U}^{k+1}) \leq \mathcal{E}_h(\mathbf{U}^k), \quad k = 0, 1, \dots, N-1.$$

Proof. Taking the discrete L^2 inner product of (3.1) with $(\mathbf{U}^{k+1} - \mathbf{U}^k)^\top$ yields

$$(3.20) \quad \begin{aligned} & \langle \mathbf{U}^{k+1} - \mathbf{U}^k, f(\mathbf{U}^{k+1}) + f(\mathbf{U}^k) \rangle - \frac{2}{\tau} \|\mathbf{U}^{k+1} - \mathbf{U}^k\|^2 \\ & + \frac{\tau}{2} h (\mathbf{U}^{k+1} - \mathbf{U}^k)^\top \mathbf{A}^{(1)} (f(\mathbf{U}^{k+1}) - f(\mathbf{U}^k)) = h (\mathbf{U}^{k+1} - \mathbf{U}^k)^\top \mathbf{A}^{(1)} (\mathbf{U}^{k+1} + \mathbf{U}^k). \end{aligned}$$

Note that $\mathbf{A}^{(1)}$ is a symmetric and positive definite matrix by Lemma 3.3, then we know that

$$(3.21) \quad (\mathbf{U}^{k+1} - \mathbf{U}^k)^\top \mathbf{A}^{(1)} (\mathbf{U}^{k+1} + \mathbf{U}^k) = (\mathbf{U}^{k+1})^\top \mathbf{A}^{(1)} \mathbf{U}^{k+1} - (\mathbf{U}^k)^\top \mathbf{A}^{(1)} \mathbf{U}^k.$$

Considering the energy function (3.18) in two adjacent time levers t_k and t_{k+1} , it is clear that

$$(3.22) \quad \begin{aligned} \mathcal{E}_h(\mathbf{U}^{k+1}) - \mathcal{E}_h(\mathbf{U}^k) &= \langle F(\mathbf{U}^{k+1}) - F(\mathbf{U}^k), \mathbf{1} \rangle \\ &+ \frac{h}{2} \left[(\mathbf{U}^{k+1})^\top \mathbf{A}^{(1)} \mathbf{U}^{k+1} - (\mathbf{U}^k)^\top \mathbf{A}^{(1)} \mathbf{U}^k \right]. \end{aligned}$$

Combining (3.20), (3.21) and (3.22) can lead to

$$\begin{aligned}
& \mathcal{E}_h(\mathbf{U}^{k+1}) - \mathcal{E}_h(\mathbf{U}^k) \\
(3.23) \quad &= \langle F(\mathbf{U}^{k+1}) - F(\mathbf{U}^k), \mathbf{1} \rangle + \frac{1}{2} \langle \mathbf{U}^{k+1} - \mathbf{U}^k, f(\mathbf{U}^{k+1}) + f(\mathbf{U}^k) \rangle \\
&\quad - \frac{1}{\tau} \|\mathbf{U}^{k+1} - \mathbf{U}^k\|^2 + \frac{\tau}{4} h (\mathbf{U}^{k+1} - \mathbf{U}^k)^\top \mathbf{B}^{(1)} (f(\mathbf{U}^{k+1}) - f(\mathbf{U}^k)).
\end{aligned}$$

It follows from the following fundamental inequalities

$$\frac{1}{4} [(\alpha^2 - 1)^2 - (\beta^2 - 1)^2] \leq (\alpha^3 - \alpha)(\alpha - \beta) + \frac{1}{2} (\alpha - \beta)^2,$$

and

$$\frac{1}{4} [(\alpha^2 - 1)^2 - (\beta^2 - 1)^2] \leq (\beta^3 - \beta)(\alpha - \beta) + \frac{1}{2} (\alpha - \beta)^2,$$

for any $\alpha, \beta \in [-1, 1]$, we get

$$\begin{aligned}
(3.24) \quad & \langle F(\mathbf{U}^{k+1}) - F(\mathbf{U}^k), \mathbf{1} \rangle = \frac{1}{4} h \sum_{j=1}^{M-1} \left[\left((U_j^{k+1})^2 - 1 \right)^2 - \left((U_j^k)^2 - 1 \right)^2 \right] \\
& \leq \frac{1}{2} h \sum_{j=1}^{M-1} \left[\left((U_j^{k+1})^3 - U_j^{k+1} \right) (U_j^{k+1} - U_j^k) \right. \\
& \quad \left. + \left((U_j^k)^3 - U_j^k \right) (U_j^{k+1} - U_j^k) + (U_j^{k+1} - U_j^k)^2 \right] \\
& = -\frac{1}{2} \langle \mathbf{U}^{k+1} - \mathbf{U}^k, f(\mathbf{U}^{k+1}) + f(\mathbf{U}^k) \rangle + \frac{1}{2} \|\mathbf{U}^{k+1} - \mathbf{U}^k\|^2.
\end{aligned}$$

Substituting (3.24) into (3.23), we further get

$$\begin{aligned}
(3.25) \quad & \mathcal{E}_h(\mathbf{U}^{k+1}) - \mathcal{E}_h(\mathbf{U}^k) \\
& \leq \left(\frac{1}{2} - \frac{1}{\tau} \right) \|\mathbf{U}^{k+1} - \mathbf{U}^k\|^2 + \frac{\tau}{4} h (\mathbf{U}^{k+1} - \mathbf{U}^k)^\top \mathbf{B}^{(1)} (f(\mathbf{U}^{k+1}) - f(\mathbf{U}^k)) \\
& \leq \left(\frac{1}{2} - \frac{1}{\tau} \right) \|\mathbf{U}^{k+1} - \mathbf{U}^k\|^2 + \frac{\tau}{4} \|\mathbf{U}^{k+1} - \mathbf{U}^k\| \|\mathbf{B}^{(1)}\| \|f(\mathbf{U}^{k+1}) - f(\mathbf{U}^k)\|.
\end{aligned}$$

Since $\|U^k\|_\infty \leq 1$ for $k = 0, 1, \dots, N$, by the mean value theorem, we know that there exist $\xi_1, \xi_2, \dots, \xi_{M-1}$, such that $|\xi_j| \leq 1$ for $j = 1, 2, \dots, M-1$ and

$$(3.26) \quad f(U_j^{k+1}) - f(U_j^k) = f'(\xi_j)(U_j^{k+1} - U_j^k), j = 1, 2, \dots, M-1.$$

Denoting $\|f'\|_{C[-1,1]} = \max_{\xi_j \in [-1,1]} |f'(\xi_j)|$. By applying the equation (3.26), we can see that

$$\begin{aligned}
(3.27) \quad & \|f(\mathbf{U}^{k+1}) - f(\mathbf{U}^k)\| = \sqrt{h \sum_{j=1}^{M-1} (f(U_j^{k+1}) - f(U_j^k))^2} = \sqrt{h \sum_{j=1}^{M-1} f'^2(\xi_j) (U_j^{k+1} - U_j^k)^2} \\
& \leq \|f'\|_{C[-1,1]} \|\mathbf{U}^{k+1} - \mathbf{U}^k\|.
\end{aligned}$$

Substituting (3.27) into (3.25) can result in

$$\begin{aligned}\mathcal{E}_h(\mathbf{U}^{k+1}) - \mathcal{E}_h(\mathbf{U}^k) &\leq \left(\frac{1}{2} - \frac{1}{\tau} + \frac{\tau}{4} \|\mathbf{A}^{(1)}\| \|f'\|_{C[-1,1]} \right) \|\mathbf{U}^{k+1} - \mathbf{U}^k\|^2 \\ &= \left(\frac{1}{2} - \frac{1}{\tau} + \frac{\tau}{4} \lambda_{\max}(\mathbf{A}^{(1)}) \|f'\|_{C[-1,1]} \right) \|\mathbf{U}^{k+1} - \mathbf{U}^k\|^2.\end{aligned}$$

Therefore, we can get the final result

$$\mathcal{E}_h(\mathbf{U}^{k+1}) \leq \mathcal{E}_h(\mathbf{U}^k), \quad k = 0, 1, 2, \dots, N-1,$$

with the help of the Lemma 3.8 and condition (3.19). This completes the proof. \square

3.5. Convergence analysis. In this section, we will give the error estimation of the fully discrete scheme (3.1) in the discrete L^∞ norm. Defining the following error function

$$\mathbf{E}^k = \mathbf{u}(x, t_k) - \mathbf{U}^k, \quad k = 0, 1, 2, \dots, N.$$

From the process of establishing the difference scheme earlier, it is not difficult to find that the truncation error of the scheme (3.1) is $R = (R_h + R_\tau) \tau$, and which given by

$$R = \mathbf{u}(x, t_{k+1}) - \mathbf{B}\mathbf{u}(x, t_k) - \frac{\tau}{2} \mathbf{g}(\mathbf{u}(x, t_{k+1})) - \frac{\tau}{2} \mathbf{B}\mathbf{g}(\mathbf{u}(x, t_k)).$$

Moreover, if the exact solution is smooth enough and belongs to $C^2([0, T]; \mathcal{C}^{6+\gamma}(\overline{\Omega}))$, then there holds that

$$\|R\|_\infty \leq (\|R_\tau\|_\infty + \|R_h\|_\infty) \tau \leq \max\{2\tau C_3, 2\tau C_4\} (\tau^2 + h^6).$$

by follows from the (2.12) and (2.15).

THEOREM 3.14. *If the exact solution of the problem (3.1) belongs to $C^2([0, T]; \mathcal{C}^{6+\gamma}(\overline{\Omega}))$ and initial value $u_0(x)$ meets $\max_{x \in \overline{\Omega}} |u_0(x)| \leq 1$. Then, we have the following error estimate for the scheme (3.1) as*

$$\|\mathbf{E}^k\|_\infty \leq 4e^T \max\{C_3, C_4\} (\tau^2 + h^6), \quad k = 0, 1, 2, \dots, N,$$

under the condition (3.7).

Proof. Subtracting (2.16) from (2.14) and taking $d = 1$, then we can get the following error equation

$$\begin{aligned}(3.28) \quad \mathbf{E}^{k+1} &= \left(\mathbf{I} + \frac{\tau}{2} \mathbf{A}^{(1)} \right)^{-1} \left(\mathbf{I} - \frac{\tau}{2} \mathbf{A}^{(1)} \right) \mathbf{E}^k + \frac{\tau}{2} [\mathbf{f}(\mathbf{u}(x, t_{k+1})) - \mathbf{f}(\mathbf{U}^{k+1})] \\ &\quad + \frac{\tau}{2} \left(\mathbf{I} + \frac{\tau}{2} \mathbf{A}^{(1)} \right)^{-1} \left(\mathbf{I} - \frac{\tau}{2} \mathbf{A}^{(1)} \right) [\mathbf{f}(\mathbf{u}(x, t_k)) - \mathbf{f}(\mathbf{U}^k)] + R.\end{aligned}$$

Reorganizing equation (3.28), it is easy to obtain

$$\begin{aligned}(3.29) \quad &\left[\left(\mathbf{I} - \frac{\tau}{2} \right) \mathbf{E}^{k+1} + \frac{\tau}{2} \left((\mathbf{U}^{k+1})^2 + \mathbf{U}^{k+1} \mathbf{u}(x, t_{k+1}) + \mathbf{u}^2(x, t_{k+1}) \right) \mathbf{E}^{k+1} \right] \\ &= \mathbf{B} \left[\left(\mathbf{I} + \frac{\tau}{2} \right) \mathbf{E}^k - \frac{\tau}{2} \left((\mathbf{U}^k)^2 + \mathbf{U}^k \mathbf{u}(x, t_k) + \mathbf{u}^2(x, t_k) \right) \mathbf{E}^k + R \right],\end{aligned}$$

where $\mathbf{B} = \left(\mathbf{I} + \frac{\tau}{2} \mathbf{A}^{(1)} \right)^{-1} \left(\mathbf{I} - \frac{\tau}{2} \mathbf{A}^{(1)} \right)$.

Considering that each element of $\left(1 - \frac{\tau}{2}\right) \mathbf{I} + \frac{\tau}{2} \left((\mathbf{U}^{k+1})^2 + \mathbf{U}^{k+1} \mathbf{u}(x, t_{k+1}) + \mathbf{u}^2(x, t_{k+1}) \right)$ is of the form $g(x, y) = \left(1 - \frac{\tau}{2}\right) + \frac{\tau}{2} (x^2 + xy + y^2)$, and a simple computation shows that

$$(3.30) \quad g_1(x, y) = \left(1 - \frac{\tau}{2}\right) + \frac{\tau}{2} (x^2 + xy + y^2) \geq 1 - \frac{\tau}{2}$$

for $x, y \in [-1, 1]$ and $0 < \tau \leq 2$. Hence, as $\|\mathbf{U}^{k+1}\|_\infty \leq 1$ and $\|u(x, t_{k+1})\|_\infty \leq 1$, it follows from (3.30) that the left-hand side of equation (3.29) can be further reduced to

$$(3.31) \quad \|\text{LHS}\|_\infty \geq \left(1 - \frac{\tau}{2}\right) \|\mathbf{E}^{k+1}\|_\infty.$$

Similarly, we can also know that

$$(3.32) \quad g_2(x, y) = \left(1 + \frac{\tau}{2}\right) - \frac{\tau}{2} (x^2 + xy + y^2) \leq 1 + \frac{\tau}{2}$$

when $x, y \in [-1, 1]$ and $\tau > 0$.

On the other hand, based on Lemma 3.6 and (3.32), the right-hand side of equation (3.29) can be estimated as

$$(3.33) \quad \begin{aligned} \|\text{RHS}\|_\infty &= \left\| \mathbf{B} \left[\left(1 + \frac{\tau}{2}\right) \mathbf{E}^k - \frac{\tau}{2} \left((\mathbf{U}^k)^2 + \mathbf{U}^k \mathbf{u}(x, t_k) + \mathbf{u}^2(x, t_k) \right) \mathbf{E}^k + R \right] \right\|_\infty \\ &\leq \left\| \left[\left(1 + \frac{\tau}{2}\right) \mathbf{I} - \frac{\tau}{2} \left((\mathbf{U}^k)^2 + \mathbf{U}^k \mathbf{u}(x, t_k) + \mathbf{u}^2(x, t_k) \right) \right] \mathbf{E}^k + R \right\|_\infty \\ &\leq \left(1 + \frac{\tau}{2}\right) \|\mathbf{E}^k\|_\infty + \max\{2\tau C_3, 2\tau C_4\} (\tau^2 + h^6) \end{aligned}$$

for $\|\mathbf{U}^k\|_\infty \leq 1$ and $\|u(x, t_k)\|_\infty \leq 1$.

Combining (3.31) and (3.33), and using the condition (3.7), then it can lead to the following result

$$\|\mathbf{E}^{k+1}\|_\infty \leq (1 + \tau) \|\mathbf{E}^k\|_\infty + \max\{4\tau C_3, 4\tau C_4\} (\tau^2 + h^6), \quad k = 0, 1, \dots, N-1.$$

Using Lemma 3.8 to the above inequality again, it is not difficult to obtain

$$\|\mathbf{E}^k\|_\infty \leq e^{\tau} \left[\|\mathbf{E}^0\|_\infty + 4 \max\{C_3, C_4\} (\tau^2 + h^6) \right], \quad k = 0, 1, \dots, N.$$

Note the fact that $\|\mathbf{E}^0\|_\infty = 0$, so the result to be proved is naturally obtained. This completes the proof. \square

4. Numerical examples. In this section, some numerical experiments are presented to demonstrate the theoretical results obtained in the previous and efficiency of the proposed numerical scheme, which are mainly divided into two parts. The first one is to test the accuracy of the numerical differential formula (2.6) with (2.7) and the fully discrete scheme (3.1), respectively. And the second part is to study the discrete maximum principle of the numerical scheme (3.1) under the time-step restriction.

4.1. Convergence order tests. In this subsection, in order to test the convergence orders for the numerical differential formula (2.6) with (2.7) and the fully discrete numerical scheme (3.1), we use exact solutions with sufficient regularity as the testing examples.

Example 4.1. Check the convergence order of the numerical differential formula (2.6) with (2.7).

TABLE 4.1
The maximum absolute errors and convergence orders of the formula (2.6) with (2.7) for $\gamma \in (1, 2]$.

γ	h	The maximum absolute errors	The convergence orders
1.1	$\frac{1}{20}$	8.755661e-008	—
	$\frac{1}{30}$	7.726314e-009	5.9873
	$\frac{1}{40}$	1.377568e-009	5.9938
	$\frac{1}{50}$	3.614164e-010	5.9963
	$\frac{1}{60}$	1.210898e-010	5.9976
1.3	$\frac{1}{20}$	1.625749e-007	—
	$\frac{1}{30}$	1.433460e-008	5.9893
	$\frac{1}{40}$	2.555080e-009	5.9948
	$\frac{1}{50}$	6.702622e-010	5.9969
	$\frac{1}{60}$	2.245534e-010	5.9979
1.5	$\frac{1}{20}$	2.921865e-007	—
	$\frac{1}{30}$	2.573720e-008	5.9918
	$\frac{1}{40}$	4.585961e-009	5.9960
	$\frac{1}{50}$	1.202822e-009	5.9976
	$\frac{1}{60}$	4.029377e-010	5.9984
1.7	$\frac{1}{20}$	5.106500e-007	—
	$\frac{1}{30}$	4.492734e-008	5.9947
	$\frac{1}{40}$	8.002056e-009	5.9974
	$\frac{1}{50}$	2.098410e-009	5.9985
	$\frac{1}{60}$	7.028819e-010	5.9990
1.9	$\frac{1}{20}$	5.106500e-007	—
	$\frac{1}{30}$	4.492734e-008	5.9947
	$\frac{1}{40}$	8.002056e-009	5.9974
	$\frac{1}{50}$	2.098410e-009	5.9985
	$\frac{1}{60}$	7.028819e-010	5.9990
2	$\frac{1}{20}$	1.125000e-006	—
	$\frac{1}{30}$	9.876543e-008	6.0000
	$\frac{1}{40}$	1.757812e-008	6.0000
	$\frac{1}{50}$	4.608001e-009	6.0000
	$\frac{1}{60}$	1.543202e-009	6.0000

Here, we choose the test function $u(x) = x^4(1-x)^4$ for $x \in (0, 1)$. Using the numerical differential formula (2.6) with (2.7) to treat this test function, and the results are shown in Table 4.1. From these numerical results, it is not difficult to find that the numerical differential formula (2.6) with (2.7) has a convergence order of 6.

In addition, in Table 4.2, we also give the results for case $\gamma \in (0, 1)$, which shown that its convergence order can also reach sixth-order. Combining Table 4.1 and Table 4.2, we can claim that the numerical numerical differential formula (2.6) with (2.7) can achieve a convergence order of sixth-order for all $\gamma \in (0, 1) \cup (1, 2]$, which is superior to existing some

numerical differential formulas, as they are only valid in the case of $\gamma \in (0, 1)$ or $\gamma \in (1, 2]$.

TABLE 4.2
The maximum absolute errors and convergence orders of the formula (2.6) with (2.7) for $\gamma \in (0, 1)$.

γ	h	The maximum absolute errors	The convergence orders
0.1	$\frac{1}{20}$	7.696507e-010	—
	$\frac{1}{30}$	6.801712e-011	5.9837
	$\frac{1}{40}$	1.213353e-011	5.9920
	$\frac{1}{50}$	3.184138e-012	5.9952
	$\frac{1}{60}$	1.066997e-012	5.9967
0.3	$\frac{1}{20}$	3.695955e-009	—
	$\frac{1}{30}$	3.266415e-010	5.9836
	$\frac{1}{40}$	5.827008e-011	5.9919
	$\frac{1}{50}$	1.529151e-011	5.9952
	$\frac{1}{60}$	5.124070e-012	5.9968
0.5	$\frac{1}{20}$	9.873718e-009	—
	$\frac{1}{30}$	8.725086e-010	5.9839
	$\frac{1}{40}$	1.556410e-010	5.9921
	$\frac{1}{50}$	4.084322e-011	5.9953
	$\frac{1}{60}$	1.368615e-011	5.9969
0.7	$\frac{1}{20}$	2.210839e-008	—
	$\frac{1}{30}$	1.953068e-009	5.9846
	$\frac{1}{40}$	3.483578e-010	5.9925
	$\frac{1}{50}$	9.141122e-011	5.9955
	$\frac{1}{60}$	3.062998e-011	5.9970
0.9	$\frac{1}{20}$	4.526141e-008	—
	$\frac{1}{30}$	3.996564e-009	5.9858
	$\frac{1}{40}$	7.127289e-010	5.9930
	$\frac{1}{50}$	1.870102e-010	5.9959
	$\frac{1}{60}$	6.266051e-011	5.9973

Example 4.2. Test the convergence order of the numerical scheme (3.1). For this purpose, we consider the following one-dimensional space fractional Allen-Cahn equation with a force term, i.e.

$$\partial_t u = \epsilon^2 \mathcal{L}^\gamma u + u - u^3 + s(x, t), \quad (x, t) \in \Omega \times (0, 1],$$

where $\Omega = [0, 1]$ and the source term is

$$\begin{aligned} s(x, t) = & e^{-3t} x^{18} (1-x)^{18} - 2e^{-t} x^6 (1-x)^6 \\ & + \frac{\epsilon^2 e^{-t}}{2 \cos\left(\frac{\pi}{2}\gamma\right)} \sum_{\ell=0}^6 \frac{(-1)^\ell 6! (6+\ell)!}{\ell! (6-\ell)! \Gamma(7+\ell-\beta)} \left[x^{6+\ell-\beta} + (1-x)^{6+\ell-\beta} \right]. \end{aligned}$$

The exact solution of the above problem is $u(x, t) = e^{-t} x^6 (1-x)^6$.

Table 4.3 shows the maximum absolute errors and convergence orders of various fractional orders, i.e., $\gamma = 1.2, 1.4, 1.6, 1.8$, at $t = 1$ by applying the numerical scheme (3.1). From the table, we can observe that the finite difference scheme (3.1) has second-order temporal accuracy and sixth-order spatial accuracy, which is in good agreement with the proven error estimates in Theorem 3.14.

TABLE 4.3

The maximum absolute error, temporal convergence order and spatial convergence order of the numerical solutions with $\epsilon = 0.001$ at $t = 1$.

γ	τ, h	The maximum absolute error	Temporal convergence order	Spatial convergence order
1.2	$\frac{1}{8}, \frac{1}{8}$	8.677284e-007	—	—
	$\frac{1}{64}, \frac{1}{16}$	1.372736e-008	1.9940	5.9821
	$\frac{1}{512}, \frac{1}{32}$	3.494463e-010	1.7653	5.2958
1.4	$\frac{1}{8}, \frac{1}{8}$	8.681616e-007	—	—
	$\frac{1}{64}, \frac{1}{16}$	1.377418e-008	1.9926	5.9779
	$\frac{1}{512}, \frac{1}{32}$	3.551702e-010	1.7591	5.2773
1.6	$\frac{1}{8}, \frac{1}{8}$	8.688534e-007	—	—
	$\frac{1}{64}, \frac{1}{16}$	1.384790e-008	1.9905	5.9714
	$\frac{1}{512}, \frac{1}{32}$	3.641537e-010	1.7497	5.2490
1.8	$\frac{1}{8}, \frac{1}{8}$	8.699670e-007	—	—
	$\frac{1}{64}, \frac{1}{16}$	1.396475e-008	1.9870	5.9611
	$\frac{1}{512}, \frac{1}{32}$	3.783460e-010	1.7353	5.2059

Furthermore, the evolutions of the error surface are also plotted in Figs. 4.1 and 4.2 for different γ . From these figures, we can find that the errors are very small, which shows that our difference scheme is effective and has high-order convergence.

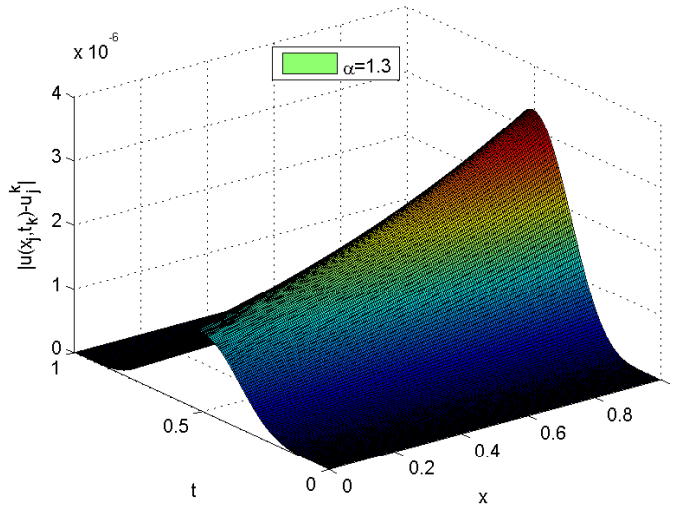


FIG. 4.1. Evolutions of the error surface for $\gamma = 1.3$ and $\epsilon = 0.005$, where $\tau = 0.005$ and $h = 0.005$.

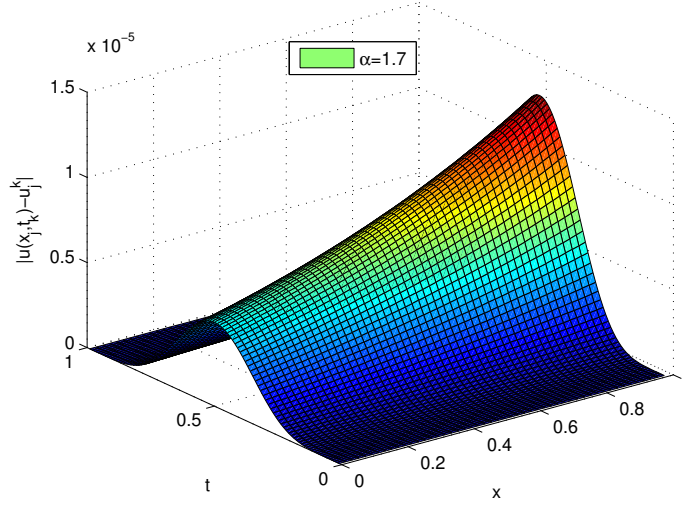


FIG. 4.2. Evolutions of the error surface for $\gamma = 1.7$ and $\epsilon = 0.01$, where $\tau = 0.02$ and $h = 0.001$.

4.2. Discrete maximum principle tests.

Example 4.3. Verify the discrete maximum principle of the numerical scheme (3.1). Here, we consider the one-dimensional space fractional Allen-Cahn equation (1.1) with the initial condition

$$u_0(x) = x^{3.5+\gamma}(1-x)^{3.5+\gamma} \sin \pi x, \quad x \in [0, 1],$$

where the zero boundary values are set for the initial condition $u_0(x)$.

For this example, we fix $h = 0.01$ and $\epsilon = 0.1$, but vary τ . The evolution graphs of the maximum values of numerical solution with different γ are given Figs. 4.3, 4.4, 4.5 and 4.6, respectively. From these figures, we can see that they are all bounded by 1, which is consistent with our theoretical analysis and further implies that condition (3.7) in Theorem 3.11 is reasonable.

5. Conclusions. In this article, based on the implicit integral factor method combined with the Padé approximation technique, we construct an efficient numerical scheme for the spatial fractional Allen-Cahn equation. Subsequently, a detailed analysis was conducted on the unique solvability of the numerical scheme under certain conditions. Furthermore, we also investigated the discrete maximum principle preservation and energy stability under the condition $0 < \tau \leq 1$. The analysis results showed that this scheme greatly weakened the limitations of existing results on the selection of time step. Meanwhile, the error analysis under the discrete L^∞ norm was also discussed in detail. Finally, a large number of numerical examples demonstrate the effectiveness of our algorithm and the correctness of theoretical analysis.

Declaration of competing interest.

The authors declare that they have no known competing financial interests or personal relationships that could have appeared to influence the work reported in this paper.

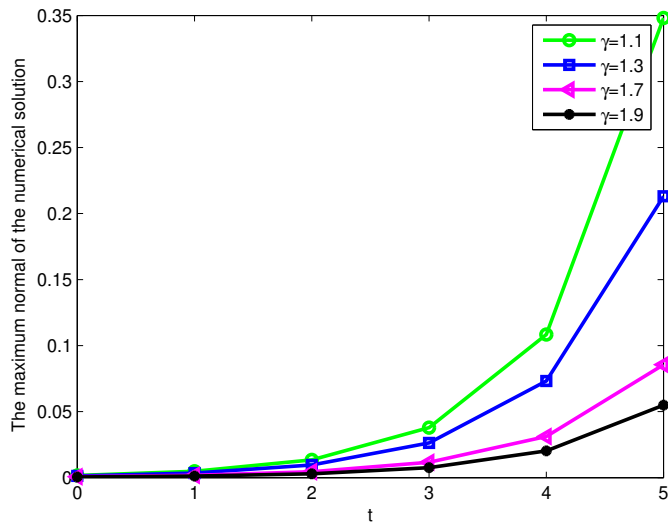


FIG. 4.3. Evolutions of the maximum norm of the numerical solutions with different γ values for $\tau = 1$.

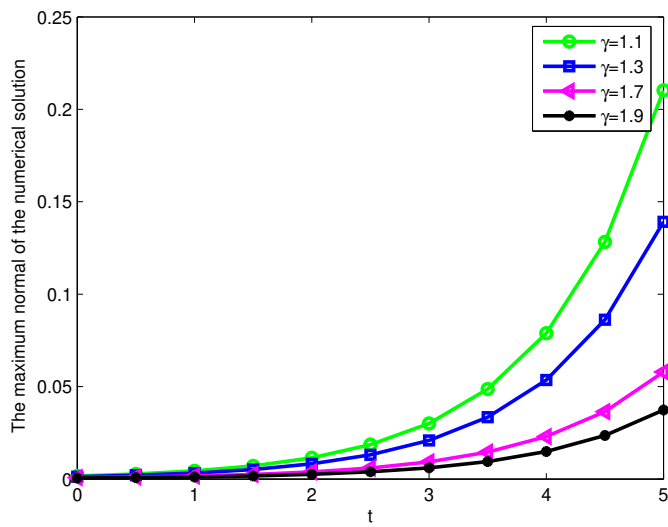


FIG. 4.4. Evolutions of the maximum norm of the numerical solutions with different γ values for $\tau = 0.5$.

Data availability.

No data was used for the research described in the article.

REFERENCES

[1] Y. NEC, A. NEPOMNYASHCHY AND A. GOLOVIN, *Front-type solutions of fractional Allen-Cahn equation*, *Physica D.*, 237 (2008), pp. 3237–3251.

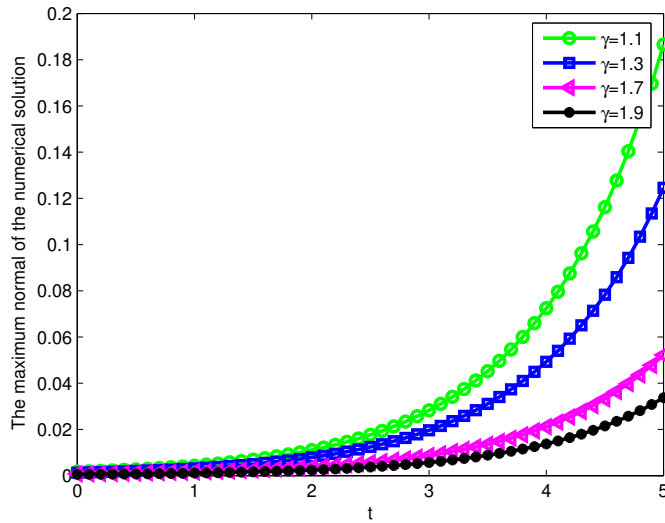


FIG. 4.5. Evolutions of the maximum norm of the numerical solutions with different γ values for $\tau = 0.1$.

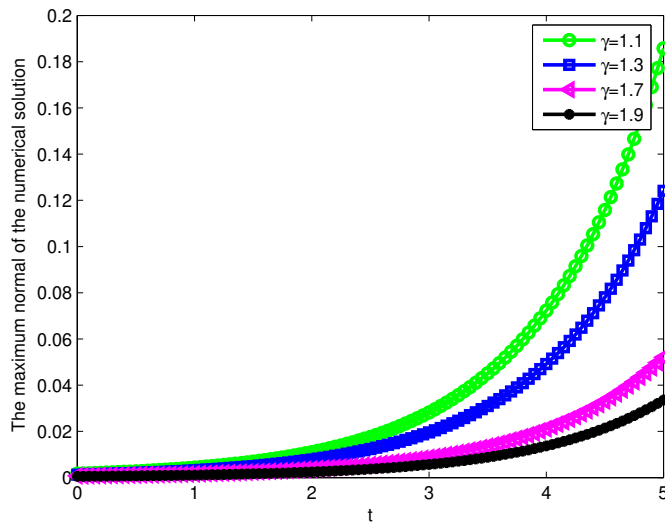


FIG. 4.6. Evolutions of the maximum norm of the numerical solutions with different γ values for $\tau = 0.05$.

- [2] I. PODLUBNY, *Fractional differential equations*. New York.: Academic Press; 1999.
- [3] T. HOU, T. TANG AND J. YANG, *Numerical analysis of fully discretized Crank-Nicolson scheme for fractional-in-space Allen-Cahn equations*, J. Sci. Comput., 72 (2017), pp. 1214–1231.
- [4] M. MEERSCHAERT, C. TADJERAN, *Finite difference approximations for fractional advection-dispersion flow equations*, J. Comput. Appl. Math., 172 (2004), pp. 65–77.
- [5] W. TIAN, H. ZHOU AND W. DENG, *A class of second order difference approximations for solving space fractional diffusion equations*, Math. Comput., 84 (2015), pp. 1703–1727.
- [6] H. ZHOU, W. TIAN AND W. DENG, *Quasi-compact finite difference schemes for space fractional diffusion equations*, J. Sci. Comput., 56 (2013), pp. 45–66.
- [7] H. DING, C. LI, *High-order numerical algorithms for Riesz derivatives via constructing new generating func-*

- tions, *J. Sci. Comput.*, 71 (2017), pp. 759–784.
- [8] C. ÇELİK, M. DUMAN, *Crank-Nicolson method for the fractional diffusion equation with the Riesz fractional derivative*, *J. Comput. Phys.*, 231 (2012), pp. 1743–1750.
- [9] M. ORTIGUEIRA, *Riesz potential operators and inverses via fractional centred derivatives*, *Int. J. Math. Sci.*, 2016 (2006), pp. 1–12.
- [10] H. DING, C. LI AND Y. CHEN, *High-order algorithms for Riesz derivative and their applications (II)*, *J. Comput. Phys.*, 293 (2015), pp. 218–237.
- [11] X. ZHAO, Z. SUN, Z. HAO, *A fourth-order compact ADI scheme for two-dimensional nonlinear space fractional Schrödinger equation*, *SIAM J. Sci. Comput.*, 2014 (2014), pp. 2865–2886.
- [12] H. DING, C. LI, *High-order algorithms for Riesz derivative and their applications (V)*, *Numer. Meth. Partial Diff. Equ.*, 33 (2017), pp. 1754–1794.
- [13] D. HE, K. PAN, H. HU, *A spatial fourth-order maximum principle preserving operator splitting scheme for the multi-dimensional fractional Allen-Cahn equation*, *Appl. Numer. Math.*, 151 (2020), pp. 44–63. (2020)
- [14] H. ZHANG, J. YAN, X. QIAN, ET AL., *On the preserving of the maximum principle and energy stability of high-order implicit-explicit Runge-Kutta schemes for the space-fractional Allen-Cahn equation*, *Numer. Algorithms*, 88 (2021), pp. 1309–1336.
- [15] Y. GONG, Y. CHEN, C. WANG, ET AL., *A new class of high-order energy-preserving schemes for the Korteweg-de Vries equation based on the quadratic auxiliary variable (QAV) approach*, *Numer. Math. Theor. Meth. Appl.*, 15 (2022), pp. 768–792.
- [16] Z. HAO, Z. ZHANG AND R. DU, *Fractional centered difference scheme for high-dimensional integral fractional Laplacian*, *J. Comput. Phys.*, 424 (2021), pp. 109851.
- [17] Z. XU, Y. FU, *Unconditional energy stability and maximum principle preserving scheme for the Allen-Cahn equation*, *Numer. Algorithms*, (2024). <https://doi.org/10.1007/s11075-024-01880-2>.
- [18] L. BU, L. MEI AND Y. HOU, *Stable second-order schemes for the space-fractional Cahn-Hilliard and Allen-Cahn equations*, *Comput. Math. Appl.*, 78 (2019), pp. 3485–3500.
- [19] H. CHEN, H. SUN, *A dimensional splitting exponential time differencing scheme for multidimensional fractional Allen-Cahn equations*, *J. Sci. Comput.*, 87 (2021), pp. 1–25.
- [20] H. CHEN, H. SUN, *Second-order maximum principle preserving Strang’s splitting schemes for anisotropic fractional Allen-Cahn equations*, *Numer. Algorithms*, (2021), pp. 1–23.
- [21] H. DING, Q. YI, *The construction of higher-order numerical approximation formula for Riesz derivative and its application to nonlinear fractional differential equations (I)*, *Commun. Nonlinear Sci.*, 110 (2022), pp. 106394.
- [22] H. DING, C. LI, *High-order numerical algorithm and error analysis for the two-dimensional nonlinear spatial fractional complex Ginzburg-Landau equation*, *Commun. Nonlinear Sci.*, 120 (2023), pp. 107160.
- [23] Q. NIE, F. WAN AND Y. ZHANG, ET AL., *Compact integration factor methods in high spatial dimensions*, *J. Comput. Phys.*, 2007 (2008), pp. 5238–5255.
- [24] C. MOLER, C. LOAN, *Nineteen dubious ways to compute the exponential of a matrix, twenty-five years later*, *SIAM Rev.*, 45 (2003), pp. 3–49.
- [25] R. CHAN, X. JIN, *An introduction to iterative Toeplitz solvers*, Philadelphia: SIAM; 2007.
- [26] R. CHAN, *Toeplitz preconditioners for Toeplitz systems with nonnegative generating functions*, *IMA J. Numer. Anal.*, 11 (1991), pp. 333–345.
- [27] D. KINCAID, W. CHENEY, *Numerical Analysis*, Brooks/Cole Pub., California, 1991.
- [28] J. HOLTE, *Discrete Grönwall lemma and applications*, In: MAA-NCS meeting at the University of North Dakota, 24 (2009), pp. 1–7.
- [29] G. AKRIVIS, *Finite difference discretization of the cubic Schrödinger equation*, *IMA J. Numer. Anal.*, 13 (1993), pp. 115–124.